



**HAL**  
open science

## Luminescent Organogels Formed by Ionic Self-Assembly of AIE- Active Phospholes

Jad Rabah, Antoine Escola, Olivier Jeannin, Pierre-Antoine Bouit, Muriel Hissler, Franck Camerel

► **To cite this version:**

Jad Rabah, Antoine Escola, Olivier Jeannin, Pierre-Antoine Bouit, Muriel Hissler, et al.. Luminescent Organogels Formed by Ionic Self-Assembly of AIE- Active Phospholes. *ChemPlusChem*, 2020, 85 (1), pp.79-83. 10.1002/cplu.201900584 . hal-02376317

**HAL Id: hal-02376317**

**<https://hal.science/hal-02376317v1>**

Submitted on 22 Nov 2019

**HAL** is a multi-disciplinary open access archive for the deposit and dissemination of scientific research documents, whether they are published or not. The documents may come from teaching and research institutions in France or abroad, or from public or private research centers.

L'archive ouverte pluridisciplinaire **HAL**, est destinée au dépôt et à la diffusion de documents scientifiques de niveau recherche, publiés ou non, émanant des établissements d'enseignement et de recherche français ou étrangers, des laboratoires publics ou privés.

---

# Luminescent Organogels Formed by Ionic Self-Assembly of AIE-Active Phospholes

Jad Rabah, Antoine Escola, Olivier Jeannin, Pierre-Antoine Bouit,\* Muriel Hissler\* and Franck Camerel\*

Dedicated to the element phosphorus on the 350th anniversary of its discovery

**Abstract:** A straightforward synthesis of molecular gelators **[1][C<sub>n</sub>Bn]** and **[1][bisC<sub>n</sub>Bn]** ( $n = 12, 16$ ) based on ionic interactions between Aggregation-Induced Emission (AIE)-active anionic phosphole and functionalized imidazolium [C<sub>n</sub>Bn] and [bisC<sub>n</sub>Bn] is described. These new molecular gelators can form luminescent organogels in various solvents. The luminescent fibers were characterized by laser scanning confocal microscope. Also, a 30 fold increase in luminescence quantum yield was observed between the diluted solution (0.6%) and the xerogel (20%) of **[1][C<sub>12</sub>Bn]**, thus highlighting the AIE effect. In these systems, the luminescence can be used to probe the dynamics of the aggregation upon solid-state phase transition and upon gelation. Solid-state investigations have also allowed to fully characterize the thermal behaviour of these ionic complexes and to extract some packing features.

The study of molecular self-assembly has increased to a matured domain of interdisciplinary research due to its highly desirable applications in material sciences, such as organic light-emitting diodes, solar cells, field-effect transistors, fluorescent imaging, and sensors.<sup>[1]</sup> Among the 3D self-assemblies, supramolecular gels have intrigued considerable attention since they exhibit stimuli-dependent physical properties. For example, combining fluorescent features with self-assembly features that generate well-ordered micro-/nanostructures, allows a control of the photoluminescence mainly by tuning the intermolecular interactions (hydrogen bonding,  $\pi$ - $\pi$  stacking interactions, Van der Waals forces...)<sup>[2]</sup> Nevertheless, some fluorophores suffer from emission quenching in the condensed phase although they emit efficiently in the solution state. Fortunately, the Aggregation-Induced Emission (AIE) effect recently appears as a promising tool to generate light in high-tech applications, especially optoelectronic and biological sensory systems.<sup>[3]</sup> The AIE phenomenon, which is opposite to the Aggregation-Caused Quenching (ACQ) process, allows light emission in condensed matter. In the AIE process, non-planar luminophores are more emissive in the aggregated state than in solution. For example, hexaphenylsiloles<sup>[3]</sup> and polyphenylphospholes<sup>[4]</sup> were found to undergo AIE. These molecules cannot pack through a  $\pi$ - $\pi$  stacking arrangement due to their propeller-like molecular structure, while the intramolecular rotations of its phenyl groups

are restricted owing to the physical constraint. This restriction of intramolecular rotations (RIR) blocks the non-radiative relaxation pathway and opens the radiative channel leading to highly emissive compounds in the condensed matter. In particular, examples of phosphole-containing organogelators were reported in the literature by T. Baumgartner *et al.*<sup>[5]</sup> These compounds were able to form emissive gels in apolar solvents with low critical gels concentrations (CCG). In all these cases, a covalent approach was used to import gelation properties on the phosphole core. Another powerful way to organize charged species into well-defined nanostructures in solid-state or in solution is based on ionic self-assembly processes (ISA).<sup>[6]</sup> For example, the combination of H-bonding with electrostatic interactions around a trisamide benzene core has allowed the formation of discotic mesogens but also to induce gelation through stacking into an extended fibrous 3D network.<sup>[7]</sup> The ISA process was also efficiently used to organize charged organic or organometallic fluorophores with commercial and synthetic amphiphiles into luminescent crystalline and soft materials.<sup>[8]</sup> In the present work, we demonstrate that anionic hydroxy-oxo-phospholes can be organized through ISA with functional imidazolium cations into structured and luminescent materials in solid-state or solution. In addition, the AIE properties of the phosphole core allow to prepare emissive organogels and to probe phase transitions in solid-state but also the dynamic of gelation processes.

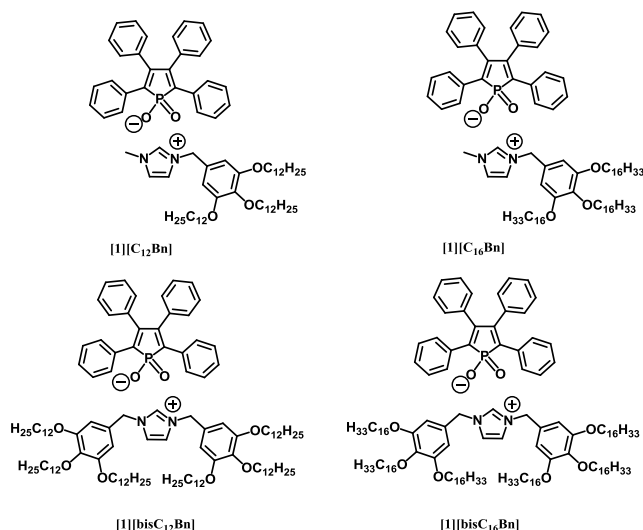
Functionalized imidazolium chloride **[C<sub>n</sub>Bn]Cl** were synthesized as previously described in the literature.<sup>[9]</sup> The anionic phospholes **[Na][1]** was prepared from the 1-hydroxy-1-oxo-2,3,4,5-tetraphenyl-phosphole<sup>[10]</sup> by simple deprotonation by NaH in THF. The complexes **[1][C<sub>n</sub>Bn]** and **[1][bisC<sub>n</sub>Bn]** ( $n = 12, 16$ ) (Scheme 1) were obtained by ionic metathesis reactions. (see SI for synthetic details). Complexation in a 1:1 ratio was unambiguously confirmed by elemental analyses and the integration of the <sup>1</sup>H-NMR spectra.

---

J. Rabah, A. Escola, Dr. O. Jeannin, Dr. P.-A. Bouit, Prof. M. Hissler, Dr. F. Camerel  
Univ Rennes, CNRS, ISCR - UMR 6226, 35000 Rennes, France.  
E-mail: pierre-antoine.bouit@univ-rennes1.fr; muriel.hissler@univ-rennes1.fr, franck.camerel@univ-rennes1.fr

Supporting information for this article is given via a link at the end of the document

---



**Scheme 1.** Structures of the ionic gelators **[1][C<sub>n</sub>Bn]** and **[1][bisC<sub>n</sub>Bn]**

Single-crystals of **[1][C<sub>12</sub>Bn]** suitable for X-ray diffraction were obtained by slow evaporation from a DCM/AcOEt solution. **[1][C<sub>12</sub>Bn]** crystallizes in the monoclinic space group  $P2_1$  (Table S1). The asymmetric unit contains two anionic phospholes and two imidazolium cations in general positions together with four water molecules. The structure unambiguously confirms the 1:1 stoichiometric ratio. The phenyl rings are all twisted out of the phosphole plane with torsion angles from  $35.6^\circ$  to  $63.6^\circ$ . The P atom is in a slightly distorted tetrahedral environment and a negatively charged oxygen atom from the P-ring is in the proximity of the imidazolium centroid ( $d = 4.29 \text{ \AA}$ ). A projection of the crystalline structure along  $a$  is presented Fig. 1a. The crystalline network is an alternation of long alkyl chains layers and phosphole units stacked in the  $a$  direction, similarly to the molecular organization of a lamello-columnar phase.<sup>[11]</sup> The packing can also be described as an alternation of apolar layers containing the carbon chains and ionic polar layers containing the imidazolium/phosphole fragments parallel to the  $(bc)$  plane. Segregation between the rigid aromatic part and the flexible carbon chains as well as electrostatic segregation seems to govern the molecular organization. A stack of the phosphole along the  $a$  axis is presented in Fig. 1b. The distance between the phosphole molecules is  $6.52 \text{ \AA}$  ( $a$  parameter), meaning that there are no  $\pi$ -stacking interactions between the fluorophores. Closer inspection of the crystalline structure reveals  $\pi$ -stacking interactions between the imidazolium units and one of the phenyl groups attached to the phosphole, leading to a 1D  $\pi$ -stack element in the structure.

The thermal properties of the ionic complexes were studied by a combination of differential scanning calorimetry (DSC) and polarizing optical microscopy (POM). Despite the presence of long carbon chains, all these compounds were found to be deprived of mesomorphic properties. The initial DSC trace of

**[1][C<sub>12</sub>Bn]** in its crystalline form displayed a broad transition ( $82.7 \text{ }^\circ\text{C}$ , Fig. S1) attributed by POM to the melting into an isotropic liquid. After cooling, the compound stays in a thermodynamically stable amorphous state and only a reversible glass transition between an amorphous liquid and an amorphous solid is detected around  $25 \text{ }^\circ\text{C}$  by DSC.

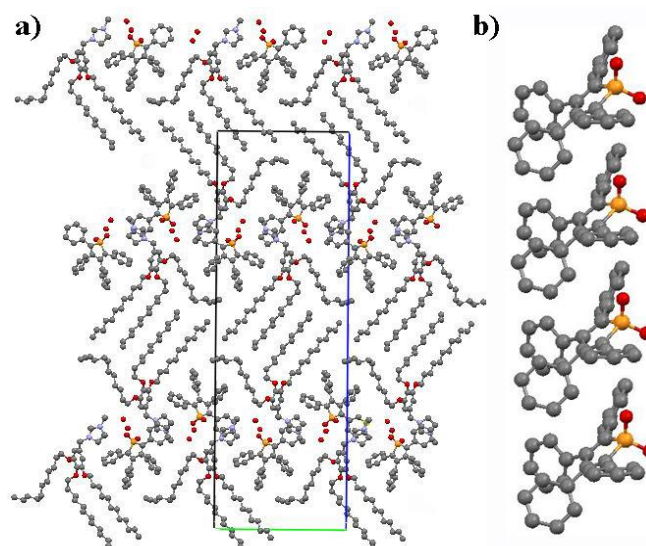


**Figure 1.** a) Projection of the crystalline structure of **[1][C<sub>12</sub>Bn]** along the  $a$  axis (H atoms have been omitted for clarity); b) Phosphole stack observed along  $a$ . CCDC 1954861 contains the supplementary crystallographic data for this paper. These data can be obtained free of charge from The Cambridge Crystallographic Data Centre.

The first heating curve of **[1][C<sub>16</sub>Bn]** also shows the melting of the compound into an isotropic liquid (Fig. S2). Upon cooling, the compound slowly crystallizes between  $40 \text{ }^\circ\text{C}$  and  $20 \text{ }^\circ\text{C}$ , as confirmed by the formation of a rigid and birefringent thin-film between crossed-polarizers. T-dependent SAXS measurements recorded upon cooling have confirmed that the two close thermal transitions observed around  $30 \text{ }^\circ\text{C}$  upon cooling at associated with an isotropic to crystal and a crystal to crystal phase transition, respectively (Figure S3). Upon further heating, two processes were detected: a first crystal-crystal phase transformation (confirmed by POM and SAXS measurements) at  $41.0 \text{ }^\circ\text{C}$  then the melting into the isotropic liquid.

The thermal behaviour of **[1][bisC<sub>12</sub>Bn]** appears more complicated (Fig S4). After a first heating above  $100 \text{ }^\circ\text{C}$ , an isotropic fluid state is formed. Upon cooling down to RT, the compound remains in an amorphous state whose viscosity increases with the decrease of  $T$ . On a second heating cycle, an exothermic peak was observed at  $79.8 \text{ }^\circ\text{C}$  indicating that the amorphous phase was metastable and the energy imported during the heating stage allowed the recrystallization in a more stable crystalline phase (Cr). On further heating, the melting into the isotropic liquid was observed ( $91.1^\circ\text{C}$ ). Such behaviour is typical of compounds with a tendency to crystallize with slow kinetics, probably induced by strong steric constraints. The formation of an amorphous state at room temperature is further

supported by the presence of a reversible glass transition around 15 °C.

After a first heating, the DSC trace of **[1][bisC<sub>16</sub>Bn]** appears simpler with a single crystal to isotropic phase transition at 47.8 °C upon heating and two close thermal transitions on the cooling curve around 35 °C which were unambiguously attributed by POM observations to an isotropic to crystal and to a crystal to crystal phase transitions (Fig. S5). Since the luminescence of the phosphole fragment should be sensitive to the viscosity/rigidity in the condensed state and especially around the crystalline to an isotropic phase transition, the luminescence intensity was recorded as a function of the temperature. For this purpose, **[1][bisC<sub>16</sub>Bn]** having a single reversible melting point was selected and the luminescence intensity was measured upon heating at 10 °C/min (Fig. 2). The luminescence intensity slowly and gradually decreases to 40 °C where a strong and rapid decrease is observed up to 50 °C. Above 50 °C, the luminescence intensity starts again to monotonously decrease. The abrupt evolution of the emission intensity is associated with the phase transition between the crystalline phase and the isotropic liquid as demonstrated by the superimposition of the DSC trace. The decrease of the luminescence intensity is not only due to a thermal quenching, which is expected to be linear with the temperature increase. The rapid decrease of the luminescence is the result of the disaggregation of the phosphole-based stacks going from the dense and compact crystalline phase to the isotropic fluid phase with reduced packing constraints. This behavior is the reverse process of the AIE. Upon cooling from the isotropic phase, a strong increase of the luminescence intensity is also observed between the isotropic phase and the crystalline state associated to the AIE process but since the phase transition upon cooling is broad and extends over a large temperature range, the luminescence intensity increase is more gradual and no sudden increase of the luminescence has been detected.

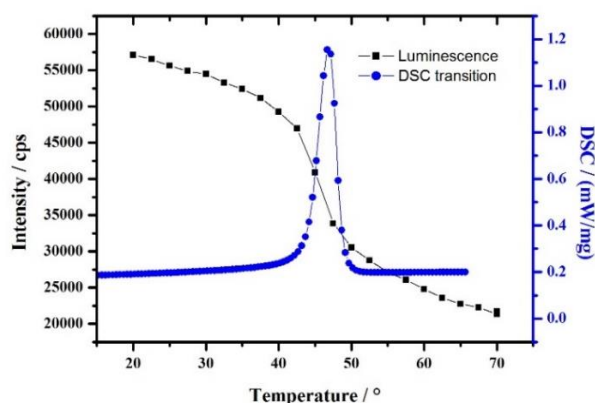


**Figure 2.** Fluorescence intensity of **[1][bisC<sub>16</sub>Bn]** as a function of the temperature and associated DSC signal.

The molecular architecture of the ionic complexes, with potential intermolecular  $\pi$ -stacking between the  $\pi$ -conjugated phosphole fragments and the aromatic parts of the cations, as well as micro-segregation due to the long alkyl chains, prompted us to evaluate

their gelation properties. Gelation of **[1][C<sub>n</sub>Bn]** / **[bisC<sub>n</sub>Bn]** ( $n = 12, 16$ ) has been evaluated in various solvents by the “stable to inversion of a test tube” method (Table S2). **[1][C<sub>12</sub>Bn]** was found to be soluble in almost all the tested solvents, except EtOAc and cyclohexane. On the contrary, **[1][C<sub>16</sub>Bn]** was almost insoluble in all the tested solvents, highlighting that small changes in the carbon chains can strongly affect the physical properties. Stable and robust gels (Fig. 3a), displaying a thermally reversible sol-to-gel phase transition, were obtained with **[1][C<sub>12</sub>Bn]** from hot n-hexane solutions at a concentration above 40 g.L<sup>-1</sup>. At this concentration, the entire volume of the solvent is immobilized and can support its own weight without collapsing. **[1][C<sub>16</sub>Bn]** with twelve additional methylene groups was found to be inefficient toward gel formation (Table S2). The gelation test results demonstrate that the obtention of a gel remains an empirical process and despite some guidelines for the gelator design the gelation properties of a molecule cannot be predicted. The yellowish gel of **[1][C<sub>12</sub>Bn]** in n-hexane appears almost transparent under white light and is highly luminescent upon UV irradiation (Fig. 3b). A clear and fluid hot solution of **[1][C<sub>12</sub>Bn]** in n-hexane (~ 55-60 °C) is almost non-luminescent under UV irradiation but the luminescence strongly increases upon cooling. (Fig. S6 and S7). This luminescence increase is attributed to the AIE during the gel formation: the molecule starts to aggregate to form the 3D network and the luminescence increase is the result of RIR (*vide infra*). It should be noticed that the **[C<sub>n</sub>Bn]Cl** ( $n = 12, 16$ ) are not able to form gels in n-hexane. Thus, the introduction of the phosphole has a crucial role in the formation of the organogel in n-hexane. The gel formation is the result of an interplay of  $\pi$ - $\pi$  stacking interactions between the phenyl groups of the phosphole and the imidazolium derivative, hydrophobic-hydrophobic segregations with the carbon chains and electrostatic interactions. The morphology of this gel was investigated by confocal microscopy. Laser scanning confocal microscope (LSCM) images were obtained from the dried gel of **[1][C<sub>12</sub>Bn]** in n-hexane (40 g.L<sup>-1</sup>) deposited on a microscope cover-slip. The images reveal an entanglement of greenish fluorescent fibers into a dense 3D network (Fig. 3). The fibers present an irregular distribution of diameters and lengths but the smallest distinguishable fibers have a mean diameter of ~ 50 nm, which is still very large compared to the molecular dimensions. This means that this fibrous structure, which is at the origin of the gel formation, turned out to be bundles of intertwining fibers with smaller diameters. The self-assembly of the ionic complexes in n-hexane into a cottony fiber-like 3D structure is thus at the origin of the gel formation. **[1][bisC<sub>16</sub>Bn]** was also able to form a gel in alcohols (Fig. S8) but only opaque and inhomogeneous gels were obtained and have not been investigated more into details.

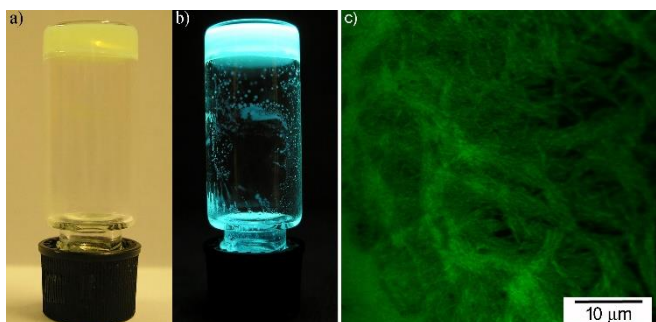


**Figure 3.** Photos of a gel of **[1][C<sub>12</sub>Bn]** in n-hexane (40 g.L<sup>-1</sup>) at RT in ambient light. (a) and under UV irradiation at 312 nm (b). LCSM images of a xerogel of **[1][C<sub>12</sub>Bn]** in n-hexane (40 g.L<sup>-1</sup>) deposited on a microscope cover slip (c)

UV-vis and fluorescence spectra of the gelator were first recorded in diluted DCM solutions (Fig. S9). The absorption spectrum of **[1][C<sub>12</sub>Bn]** displays a classical phosphole-like  $\pi$ - $\pi^*$  transition at 365 nm.<sup>[12]</sup> **[1][C<sub>12</sub>Bn]** displays a large emission band around 500 nm, also typical of the  $\pi$ -extended system. The luminescence quantum yield  $\Phi_f$  in diluted DCM was found to be weak (0.6 %). As expected for such AIE-active compounds, a larger  $\Phi_f$  for **[1][C<sub>12</sub>Bn]** was measured in solid-state (16 %). Similarly, a  $\Phi_f$  of 17 % and 20 % were measured on the gel and the xerogel of **[1][C<sub>12</sub>Bn]**, respectively. The large quantum yields measured in gel state which are comparable to the solid-state and thus considerably higher than the diluted solution, indicate that AIE efficiently takes place in the gel. The emission wavelength in the three states (solution, gel, and solid) is classical for RIR-based AIE-active compounds. No shift of the emission was observed between the solution, the solid and the gel state, highlighting the absence of phosphole-phosphole interactions (Figure S10), as observed in the crystallographic structure.

As mentioned, the luminescence strongly evolved during the gelation on going from a weakly luminescent solution to a highly emissive gel. It was recently demonstrated that changes in the emission can efficiently be used to probe the hierarchy of gelation.<sup>[13]</sup> For this purpose, a suspension of **[1][C<sub>12</sub>Bn]** in n-hexane (40 g.L<sup>-1</sup>) was refluxed until a clear solution was obtained and the emission spectra were recorded upon cooling down (Fig. 5). As expected, the luminescence intensity of **[1][C<sub>12</sub>Bn]** increases upon cooling from 0 min ( $T \approx 68^\circ\text{C}$ ) to 45 min (RT) during the gel formation (Fig. 5). Again, the strong luminescence increase is associated with the AIE during the gel formation. In fact, in the gel state, the molecules are confined into a fibrous 3D network and thus the RIR leads to a highly emissive gel compare to the solution state, as previously observed with the  $\Phi_f$  values.

The evolution of the luminescence intensity was also plotted as a function of the time (Fig. S11). The luminescence intensity globally increases upon gelation. However, the evolution is non-monotonous and several regimes can be distinguished. The complexity of the luminescence evolution highlights that the formation of the 3D network at the origin of the gelation arises through a highly dynamic hierarchical process likely involving various nucleation and growth phases.

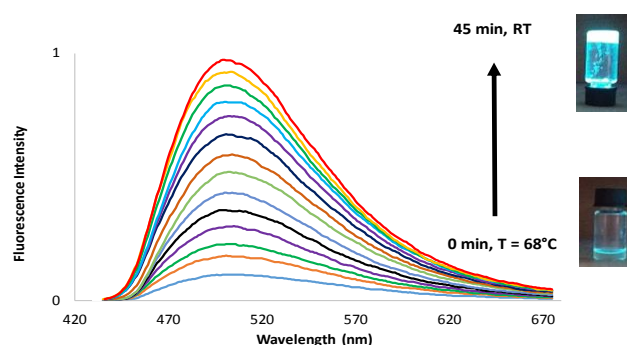


**Figure 4.** Time-dependent emission spectra measured upon cooling a hot solution of **[1][C<sub>12</sub>Bn]** at 40 g.L<sup>-1</sup> in n-hexane, to RT ( $\lambda_{ex} = 350$  nm).

To conclude, the ionic associations of a charged AIE-active phosphole moiety with functional imidazolium carrying long carbon chains have allowed its facile organization in solid-state and solution. The AIE effect was found to be highly effective in the condensed state. This effect can be used to probe the extent, the dynamic of the aggregation behaviour upon phase transition and gelation. An increase of the luminescence properties was observed on going from the fluid isotropic phase to the solid crystalline material. A strong luminescence increase was also observed during the gelation process of **[1][C<sub>12</sub>Bn]** in hexane. The luminescence increase is in line with the increase of the aggregation of the phosphole moiety. The formation of a luminescent cottony fiber-like 3D network is responsible for the observed gelation. This work nicely demonstrates that the ISA strategy applied to ionic AIE-active luminophores easily gives access to highly responsive molecular systems which can be useful for the future development of sensors or active-nanostructures for optoelectronic applications.

## Acknowledgements

This work is supported by the Ministère de la Recherche et de l'Enseignement Supérieur, the CNRS, the Région Bretagne, the French National Research Agency (ANR Heterographene ANR-16-CE05-0003-01, ANR Fluohyb ANR-17-CE09-0020), and the China-French associated international laboratory in "Functional Organophosphorus Materials".

## Conflict of interest

The authors declare no conflict of interest.

**Keywords:** aggregation-induced emission • gels • imidazolium • ionic self-assembly • phospholes

- 
- [1] a) S. S. Babu, V. K. Praveen, A. Ajayaghosh, *Chem. Rev.* **2014**, *114*, 1973-2129; b) S. Banerjee, R.K. Das, U. Maitra, *J. Mater. Chem.* **2009**, *19*, 6649-6687; c) A. B. Marco, F. Aparicio, L. Faour, K. Iliopoulos, Y. Morille, M. Allain, S. Franco, R. Andreu, B. Sahraoui, D. Gindre, D. Canevet, M. Sallé, *J. Am. Chem. Soc.* **2016**, *138*, 9025-9028.
- [2] a) S. Banerjee, R.K. Das, U. Maitra, *J. Mater. Chem.* **2009**, *19*, 6649-6687; b) R.G. Weiss, P. Terech, *Molecular Gels, Materials With Self-Assembled Fibrillar Networks*, Springer, Dordrecht, **2006**.
- [3] a) Y. Hong, J. W. Y. Lam, B. Z. Tang, *Chem. Soc. Rev.* **2011**, *40*, 5361-5388; b) J. Mei, N. L. C. Leung, R. T. K. Kwok, J. W. Y. Lam, B. Z. Tang, *Chem. Rev.* **2015**, *115*, 11718-11940; c) B.-K. An, J. Gierschner, S. Y. Park, *Acc. Chem. Res.* **2012**, *45*, 544-554; d) X. Wang, Z. Ding, Y. Ma, Y. Zhang, H. Shang, S. Jiang, *Soft Matter* **2019**, *15*, 1658-1665.
- [4] a) H. Su, O. Fadhel, C.-J. Wang, T.-Y. Cho, C. Fave, M. Hissler, C.-C. Wu, R. Réau, *J. Am. Chem. Soc.* **2006**, *128*, 983-995. b) F. Bu, E. Wang, Q. Peng, R. Hu, A. Qin, Z. Zhao, B. Z. Tang, *Chem. Eur. J.* **2015**, *21*, 4440-4449; c) K. Shiraishi, T. Kashiwabara, T. Sanji, M. Tanaka, *New J. Chem.* **2009**, *33*, 1680-1684; d) A. Fukazawa, Y. Ichihashi, S. Yamaguchi, *New J. Chem.* **2010**, *34*, 1537-1540; e) F. Riobé, R. Szűcs, P.-A. Bouit, D. Tondelier, B. Geffroy, F. Aparicio, J. Buendía, L. Sánchez, R. Réau, L. Nyulászi, M. Hissler, *Chem. Eur. J.* **2015**, *21*, 6547-6556; f) P. Bolle, Y. Chéret, C. Roiland L. Sanguinet, E. Faulques, H. Serier-Brault, P.-A. Bouit, M. Hissler, R. Dessapt, *Chem. Asian J.* **2019**, *14*, 1642-1646.
- [5] a) Y. Ren, W. H. Kan, V. Thangadurai, T. Baumgartner, *Angew. Chem. Int. Ed.* **2012**, *51*, 3964-3968; b) X. He, J. B. Lin, W. H. Kan, P. Dong, S. Trudel, T. Baumgartner, *Adv. Funct. Mater.* **2014**, *24*, 897-906; c) Z. Wang, B. S. Gelfand, T. Baumgartner, *Angew. Chem. Int. Ed.* **2016**, *55*, 3481-3485; d) C. Romero-Nieto, M. Marcos, S. Merino, J. Barberá, T. Baumgartner, J. Rodríguez-López, *Adv. Funct. Mater.* **2011**, *21*, 4088-4099.
- [6] a) C. F. J. Faul, M. Antonietti, *Adv. Mater.* **2003**, *15*, 673-683; b) C. F. J. Faul, *Acc. Chem. Res.* **2014**, *47*, 3428-3438.
- [7] F. Camerel, C.F.J. Faul, *Chem. Comm.* **2003**, 1958-1959.
- [8] a) F. Camerel, G. Ulrich, J. Barbera, R. Ziessel, *Chem. Eur. J.* **2007**, *13*, 2189-2200; b) F. Camerel, J. Barbera, J. Otsuki, T. Tokimoto, Y. Shimazaki, L.-Y. chen, S.-H. liu, M.-S. Lin, C.-C. Wu, R. Ziessel, *Adv. Mater.* **2008**, *20*, 3462-3467; c) J.-H. Olivier, F. Camerel, J. Barbera, P. Retailleau, R. Ziessel, *Chem. Eur. J.* **2009**, *15*, 8163-8174; d) F. Camerel, A. Vacher, O. Jeannin, J. Barbera, M. Fourmigué, *Chem. Eur. J.* **2015**, *21*, 19149-19158.
- [9] a) J.-H. Olivier, F. Camerel, G. Ulrich, J. Barbera, R. Ziessel, *Chem. Eur. J.* **2010**, *24*, 7134-7142; b) J.-H. Olivier, F. Camerel, J. Barbera, P. Retailleau, R. Ziessel, *Chem. Eur. J.* **2009**, *15*, 8163-8174; c) H. Ohta, T. Fujihara, Y. Tsuji, *Dalton Transactions* **2008**, *3*, 379-385.
- [10] a) L. D. Freedman, B. R. Ezzel, R. N. Jenkins, R. M. Harris, *Phosphorus* **1974**, *4*, 199; b) J. Ackermann, O. Margeat, M. Hissler, P.-A. Bouit, *PCT Int. Appl.* **2015**, WO 2015124802 A1 20150827.
- [11] F. Camerel, B. Donnio, C. Bourgogne, M. Schmutz, D. guillon, P. Davidson, R. Ziessel, *Chem. Eur. J.* **2006**, *12*, 4261-4274.
- [12] M. P. Duffy, W. Delaunay, P.-A. Bouit, M. Hissler, *Chem. Soc. Rev.* **2016**, *45*, 5296-5310.
- [13] Q. Benito, A. Fargues, A. Garcia, S. Maron, T. Gacoin, J.-P. Boilot, S. Perruchas, F. Camerel, *Chem. Eur. J.* **2013**, *19*, 15831-15835.
-